

Trapping of Methylglyoxal by Curcumin in Cell-Free Systems and in Human Umbilical Vein Endothelial Cells

Te-Yu Hu,^{†,||} Cheng-Ling Liu,^{†,||} Charng-Cherng Chyau,^{*,§} and Miao-Lin Hu^{*,†,‡}

[†]Department of Food Science and Biotechnology and [‡]Agricultural Biotechnology Center, National Chung Hsing University, Taichung, Taiwan 402

[§]Department of Biotechnology, Hungkuang University, Taichung, Taiwan 433

ABSTRACT: Curcumin, the most active compound of curcuminoids, has been shown to inhibit formation of advanced glycation end products (AGEs) in streptozotocin-induced diabetic rats. However, little is known on whether curcumin may trap methylglyoxal (MGO), a major reactive dicarbonyl compound, to inhibit AGE formation. We found that one molecule of curcumin effectively trapped one molecule of MGO at a 1:3 ratio at 24 h of incubation under physiological conditions (pH 7.4, 37 °C). Curcumin decreased *N*^ε-(carboxymethyl)lysine (CML) expression in human umbilical vein endothelial cells. We further used two curcumin analogues, dimethoxycurcumin (DIMC) and ferulic acid, to investigate the possible MGO-trapping mechanism of curcumin. Results reveal that DIMC, but not ferulic acid, exhibited MGO-trapping capacity, indicating curcumin traps MGO at the electron-dense carbon atom (C10) between the two keto carbon groups. Thus, curcumin may prevent MGO-induced endothelial dysfunction by directly trapping MGO.

KEYWORDS: methylglyoxal, advanced glycation end products, curcumin, HUVECs

■ INTRODUCTION

Epidemiological studies have indicated that hyperglycemia is the most important factor in diabetic complications, especially in type 2 diabetes mellitus.¹ Hyperglycemia-induced formation of advanced glycation end products (AGEs) is considered the main cause of diabetes-related complications, including retinopathy, nephropathy, neuropathy, and atherosclerosis.² AGEs are formed through the nonenzymatic glycation reaction, also called the Maillard reaction, in which the free amino group of the protein is irreversibly modified by the carbonyl group of the reducing sugars,³ followed by an Amadori rearrangement to form the stable Amadori product.⁴ In addition, the autoxidation of glucose and lipid peroxidation are also important sources of reactive dicarbonyl species (RCOS),^{5,6} which are the pivotal intermediates in the formation of AGEs *in vivo*.⁷

A major RCOS in the human body is methylglyoxal (MGO), a precursor of AGEs. Plasma levels of MGO are elevated in diabetes, dialysis, and chronic kidney disease of patients. For example, the concentration of MGO in plasma of diabetic patients is 2.2–3.8 μM, whereas the concentration of MGO in healthy volunteers is 0.4–1.0 μM.⁸ MGO can be produced by glycolysis,⁹ the sorbitol pathway,⁹ lipid peroxidation,¹⁰ catabolism of threonine,¹¹ and metabolism of ketone bodies.¹² Free MGO can react irreversibly with lysine and arginine residues of protein to form fluorescent and cross-linking AGEs, such as 1,3-di-*N*^ε-lysino-4-methylimidazolium,¹³ and nonfluorescent/non-cross-linking AGEs, including *N*^ε-(carboxymethyl)lysine (CML)¹⁴ and argpyrimidine.¹⁵ Several dietary flavonoids have been shown to inhibit AGE formation though blocking the carbonyl or dicarbonyl groups and thus may prevent diabetes and its complications.

The principal curcuminoid of the popular Indian spice turmeric, such as curcumin, demethoxycurcumin, and bisdemethoxycurcumin, are rich in the root of the *Curcuma longa*, a

member of the ginger family (Zingiberaceae).¹⁶ Among these curcuminoids, curcumin has been shown to have many biological functions, such as antioxidant,¹⁷ anti-inflammatory,¹⁸ and anticancer¹⁹ activities and to act as a potential agent against various chronic diseases such as diabetes.²⁰ Importantly, curcumin has been shown to inhibit protein glycation in erythrocytes and the formation of AGE as well as cross-linking of collagen in diabetic animals.²¹ However, little is known on whether inhibition of AGE formation by curcumin is attributable to its MGO-trapping capacity. In the present study, we investigated the trapping capacity of curcumin using HPLC and determined the formation of curcumin–MGO adducts using HPLC/ESI-MS–MS under physiological conditions (pH 7.4, 37 °C). We further employed two curcumin analogues, dimethoxycurcumin (DIMC) and ferulic acid, to investigate the possible mechanism of MGO-trapping by curcumin using HPLC/MS–MS. In addition, we used human umbilical vein endothelial cells (HUVECs) as the cell model to determine the effects of curcumin on MGO-trapping capacity.

■ MATERIALS AND METHODS

Materials. Curcumin (with a purity of ≥98%, as claimed by the supplier and determined in our laboratory using HPLC) was purchased from the Tianjin Zhongxin Pharmaceutical Research and Design Center (China). MGO (1.45 mM), 2-methylquinoxaline (2-MQ), 5-methylquinoxaline (5-MQ), 1,2-diaminobenzene (DB), and ferulic acid were purchased from Sigma (St. Louis, MO). HPLC-grade acetic acid and acetonitrile were purchased from Panreac (Barcelona, Spain) and Li Chrosolv (Whitehouse Station, NJ). DIMC and ferulic acid (with a purity of ≥98%, as claimed by the supplier) was obtained

Received: May 18, 2012

Revised: July 31, 2012

Accepted: July 31, 2012

Published: July 31, 2012



from Laila Impex (Vijayawada, India). CML antibody was purchased from Biotest International (Saco, ME).

Cell Cultures and Cell Proliferation. HUVECs were obtained from the Food Industry Research and Development Institute (FIRDI; Taiwan) and cultured in M199 medium (Invitrogen) containing 20% (v/v) fetal bovine serum (FBS), 1.5 g/L NaHCO₃, 2 mM L-glutamine, 30 μg/mL (–)-epigallocatechin-3-gallate (EGCG), penicillin (100 kU/L), and streptomycin (100 kU/L) in a humidified incubator under 5% CO₂ and 95% air at 37 °C. The cell proliferation was measured using the 3-(4,5-dimethylthiazol-2-yl)-2,5-diphenyltetrazolium bromide assay, as described previously.²²

Determination of the MGO-Trapping Capacity of Curcumin and Curcumin Analogues by HPLC. The chemical structures of curcumin, DIMC, and ferulic acid are shown in Figure 1. A mixture of

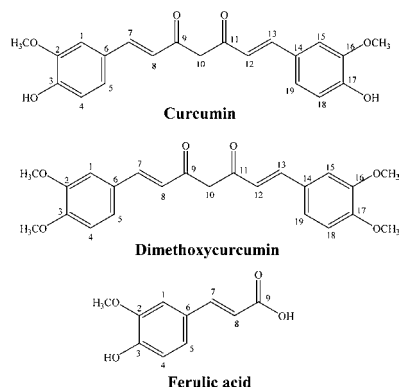


Figure 1. Structures of curcumin, DIMC, and ferulic acid.

MGO (1.45 mM) with curcumin (0.48 mM, 0.73 mM, 1.45 mM), DIMC (0.48 mM), or ferulic acid (0.48 mM) in phosphate buffer solution (pH 7.4) at 37 °C was shaken at 40 rpm for 0–72 h. Because MGO coeluted with the mobile phase, this carbonyl was allowed to react with DB (30 mM) for 1 h to form stable 2-MQ for reliable quantification.²³ The amount of 2-MQ derived from residual MGO and DB was monitored using HPLC with 5-MQ as the internal standard. The percentage of MGO reduction was calculated using the equation: reduction (%) = [(amount of MGO in control – amount of MGO in test compound)/amount of MGO in control] × 100.²⁴ The level of MQ was analyzed using HPLC associated with a Hitachi L-7100 chromatography pump and a diode array detector (Hitachi, Japan). A reversed-phase column Phenomenex Luna C18 column (4.6 mm i.d. × 250 mm, 5 μm particle size) was used. HPLC was performed under binary gradient elution, which contained mobile phases A (distilled water containing 0.2% acetic acid) and B (100% acetonitrile). All solvents were filtered through a 0.2 μm Nylaflo membrane filter. The flow rate was maintained at 1 mL/min. A linear gradient elution was carried out with 8–95% mobile phase B for 9 min and then with 95% mobile phase B for 1 min. The injection volume was 20 μL for each sample solution, and the wavelength of the UV detector was set at 313 nm for MQ. A linear equation, $y = 0.075x + 0.0051$, was obtained using MGO as the standard.

Formation of MGO Adducts of Curcumin Using HPLC/MS–MS Analysis. A mixture of curcumin (0.48 mM) with MGO (1.45 mM) in phosphate buffer solution (pH 7.4) was shaken at 40 rpm for 24 h at 37 °C, followed by immediate analysis using HPLC/ESI–MS–MS. The HPLC/electrospray ionization (ESI) mass spectrometric analysis of curcumin and its related degraded compounds was performed as described previously^{25,26} with minor modification. In brief, curcumin–MGO adducts was conducted on a Phenomenex Luna C18 column (2.00 mm i.d. × 150 mm, 3.0 μm particle size) using an HPLC system that consisted of a Finnigan Surveyor module separation system and a photodiode-array (PDA) detector (Thermo Electron Co., Waltham, MA). The elution solvent system was performed by gradient elution using two solvents: solvent A (water containing 0.1% formic acid) and solvent B (acetonitrile containing

0.1% formic acid). The flow rate during the elution process was 0.2 mL/min. A linear gradient elution was carried out with 30–95% B for 30 min and then with 95% B isocratic elution for 5 min. The absorption spectra of eluted compounds were scanned within 190–600 nm using the in-line PDA detector monitored at 230, 280, and 425 nm, respectively. The compounds having been eluted and separated were further identified with a Finnigan LCQ Advantage MAX ion trap mass spectrometer. The system was operated in ESI with a negative ionization mode. The typical operating parameters were as follows: spray needle voltage, 3.5 kV; capillary voltage, –16 V; tube lens offset, –55 V; ion transfer capillary temperature, 320 °C; nitrogen sheath gas, 45 (arbitrary units); auxiliary gas, 5 (arbitrary units). Mass spectra were acquired in the m/z range of 150–600, with five microscans and a maximum ion injection time of 200 ms. A sample volume of 20 μL was directly injected into the column using a Rheodyne (model 7725i) injection valve. In addition, the ESI–MS–MS conditions were as follows: helium was used as the damping and collision gas, and the collision energy was 35 V.

Determination of Intracellular MGO Levels. Intracellular MGO levels were analyzed using HPLC, as described previously.²⁷ In brief, the cells were washed twice and scraped into phosphate-buffered saline (PBS). After sonication, the homogenate was used for MGO level analysis and protein determination. MGO was derivatized with DB to form 2-MQ, for which the homogenate was incubated in the dark with perchloric acid (0.45 N final concentration) and DB (10 mM final concentration) for 24 h at room temperature. The levels of 2-MQ and the internal standard (5-MQ) were measured by an HPLC system, as described above. The intracellular MGO concentrations were calculated by a standard curve of MGO (0–10 μM). Values of the limit of detection (LOD = 0.22 μM) and limit of quantification (LOQ = 0.73 μM) were obtained on the basis of the equations $LOD = 3.3\delta/S$ and $LOQ = 3.3(LOD)$, where δ is the standard deviation of the intercept and S is the slope from the linear equation of the standard curve: $y = 0.075x + 0.0051$ ($R^2 = 0.9999$). Intracellular MGO levels were expressed as nanomoles of MGO per milligram of protein. The protein levels were determined by Coomassie blue (Bradford, Richmond, CA).

Determination of the Protein Levels of CML in HUVECs Using Western blotting. Protein expression of CML was measured by Western blotting. In cell culture experiments, the medium was removed and cells were rinsed with PBS twice. After the addition of 0.5 mL of cold radioimmunoprecipitation assay (RIPA) buffer and protease inhibitors, cells were scraped and mildly vortexed at 0 °C for 20 min, and the cell lysates were then subjected to centrifugation (10000g for 30 min at 4 °C). An amount of protein (50 μg) from the supernatant was resolved on sodium dodecyl sulfate–polyacrylamide gel electrophoresis (SDS–PAGE) and transferred onto a poly(vinylidene fluoride) (PVDF) membrane. After blocking with Tris-buffered saline (TBS) (20 mmol/L Tris–HCl, 150 mmol/L NaCl, pH 7.4) containing 5% nonfat milk, the membrane was incubated with monoclonal antibody against human CML, followed by incubation with horseradish peroxidase-conjugated antigoat immunoglobulin G (IgG), and then visualized using an ECL chemiluminescent detection kit (Amersham, Sweden). The relative density of the immunoreactive bands was quantified by densitometry (Gel Pro Analyzer TM, version 3.0, Media Cybernetics, Rockville, MD).

Statistical Analysis. All experiments were repeated at least three times. Values are expressed as means ± SD and analyzed using one-way analysis of variance (ANOVA) followed by a least significant difference (LSD) test for comparisons of group means. All statistical analyses were performed using SPSS for Windows, version 10 (SPSS, Inc.); a P value of <0.05 is considered statistically significant.

RESULTS AND DISCUSSION

MGO-Trapping Capacity of Curcumin. Recently, some trapping agents of reactive dicarbonyl species from dietary sources, such as tea polyphenol EGCG,³ apple polyphenols phloretin and phloridzin,²⁸ cinnamon proanthocyanidins,²⁹ phlorotannins from brown algae (*Fucus vesiculosus*),³⁰ and

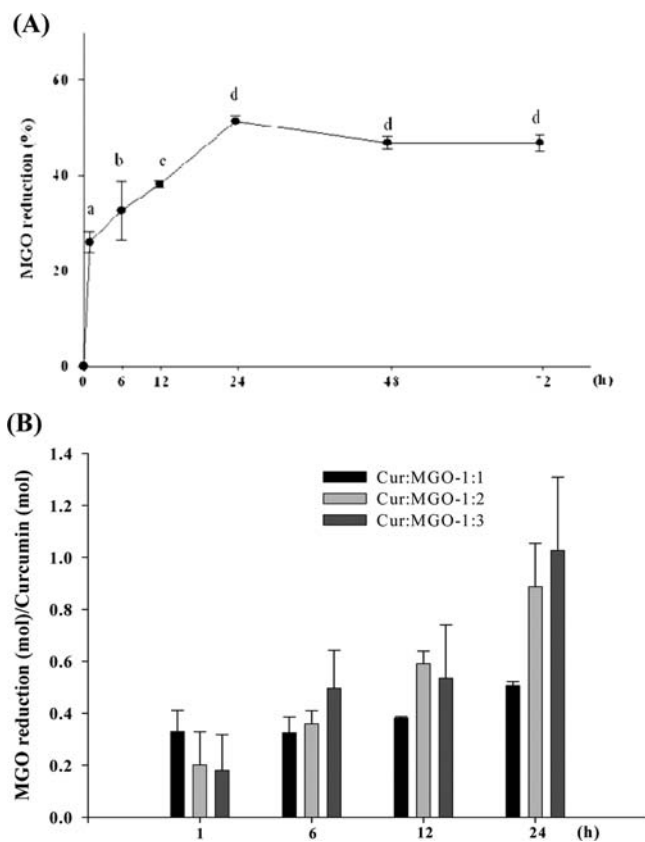


Figure 2. MGO-trapping capacity of curcumin under physiological conditions (pH 7.4, 37 °C). Curcumin (1.45 mM) was incubated with MGO (1.45 mM) for up to 72 h (A). Effect of curcumin at different ratios of curcumin to MGO (1:1, 1:2, and 1:3) on MGO-trapping capacity (B). Curcumin (0.48, 0.73, and 1.45 mM) was incubated with MGO (1.45 mM) for 1–24 h. Values are means \pm SD, $n = 3$; means without a common letter differ, $P < 0.05$.

Table 1. Retention Time and UV–Vis and Mass Spectral Characteristics for Curcumin and the Related Degradation Compounds^a

peak	compound	t_R^b (min)	UV λ_{max} (nm)	MW ^c	(–)-ESI-MS ^d m/z	(–)-ESI-MS ^d m/z (rel intens)
1	curcumin–MGO	11.42	425, 275, 236	440	439	421 (100), 271 (57)
2	unknown	17.65	455, 170, 246 sh, 299	550	549	491 (100), 327 (53), 369 (38)
3	curcumin	20.05	429, 266, 237	368	367	217 (100), 175 (48)

^aAfter incubation of curcumin (0.48 mM) with MGO (1.45 mM) in phosphate buffer solution (pH 7.4) at 37 °C for 24 h, the samples were immediately analyzed using HPLC/ESI-MS–MS. ^b t_R = retention time. ^cMW = molecular weight. ^dESI-MS = electrospray ionization mass spectrometry.

stilbene glucoside from *Polygonum multiflorum* Thunb.,³¹ have been shown to possess MGO-trapping capacity. In this study, we found that curcumin significantly and time-dependently trapped MGO under physiological conditions for up to 24 h (51% reduction, $P < 0.05$), and the effect remained unchanged for up to 72 h of incubation (Figure 2A). We then determined how many molecules of MGO could be trapped by one molecule of curcumin by using different ratios of curcumin to MGO (1:1, 1:2, 1:3). The results reveal that one molecule of curcumin trapped approximately one molecule of MGO at 1:2 and 1:3 ratios at 24 h of incubation (Figure 2B).

Curcumin–MGO Adduct Formation. We further identified the curcumin–MGO adducts using HPLC/ESI-MS–MS after incubation of curcumin with MGO at a 1:3 ratio for 24 h. As shown in Figure 3A, three major peaks were observed, with retention times of 11.42, 17.65, and 20.05 min. Data suggest that peak 3 is curcumin, as evidenced by the same retention time of pure curcumin (Figure 3B) and the molecular ion m/z 367 ($[M - H]^-$) (Table 1). In addition, the MS–MS spectrum

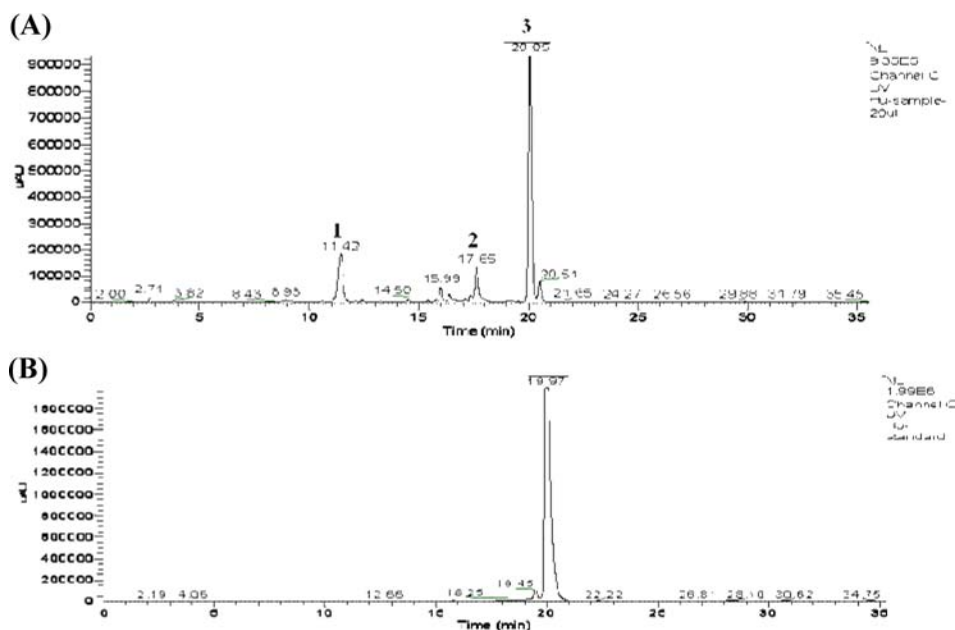


Figure 3. HPLC/UV chromatogram of the product of curcumin incubated with MGO at a 1:3 ratio for 24 h (A) and pure curcumin (B). The curcumin-related compounds correspond to peaks 1–3.

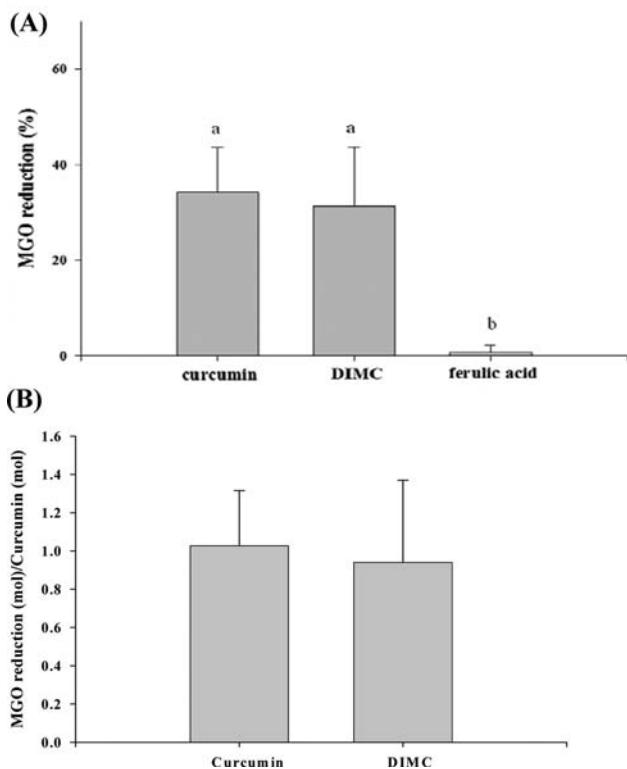


Figure 4. Effect of curcumin analogues on the MGO-trapping capacity under physiological conditions (pH 7.4, 37 °C): (A) MGO-trapping capacity (%) of curcumin, DIMC, and ferulic acid under physiological conditions (pH 7.4, 37 °C), (B) molecular ratio of the MGO-trapping capacity of curcumin and DIMC at 37 °C for 24 h of incubation. Values are means \pm SD, $n = 3$; means without a common letter differ, $P < 0.05$.

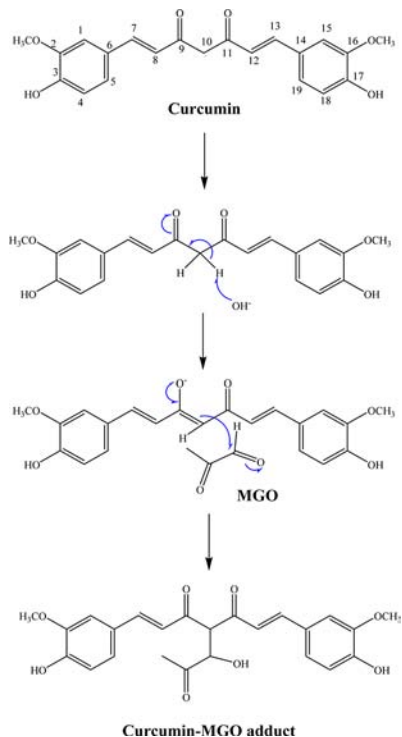


Figure 5. Proposed formation pathway of curcumin–MGO adducts under physiological conditions (pH 7.4, 37 °C).

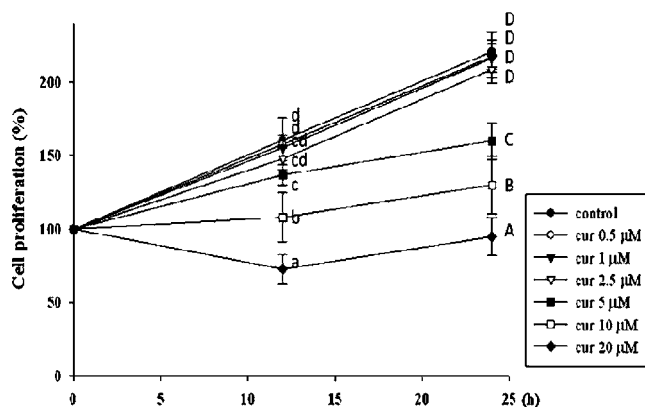


Figure 6. Effect of curcumin (0–20 μ M) on cell proliferation in HUVECs incubated for 12 and 24 h. Values are means \pm SD, $n = 3$; means without a common letter differ significantly, $P < 0.05$.

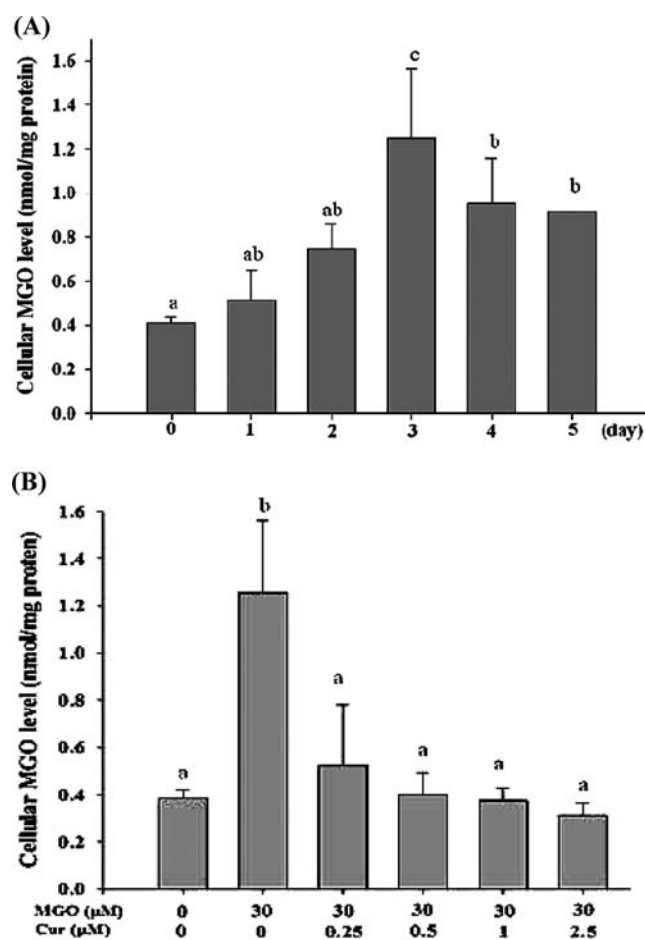


Figure 7. (A) Intracellular MGO in HUVECs incubated with MGO (30 μ M) at 37 °C for 0–5 days. (B) Level of intracellular MGO in HUVECs pretreated with curcumin (0.25–2.5 μ M) for 24 h followed by incubation with MGO (30 μ M) for 3 days. Values are means \pm SD, $n = 3$; means without a common letter differ significantly, $P < 0.05$.

of the molecular ion m/z 367 of curcumin was m/z 217 and 175, which are consistent with those of a previous study.²⁶ These results suggest that curcumin may lose a neutral moiety to generate the fragment ion m/z 217 ($[M - 150 - H]^-$) via a β -hydrogen shift to the double bond of one of the diketones of deprotonated curcumin.³² Curcumin may also generate the

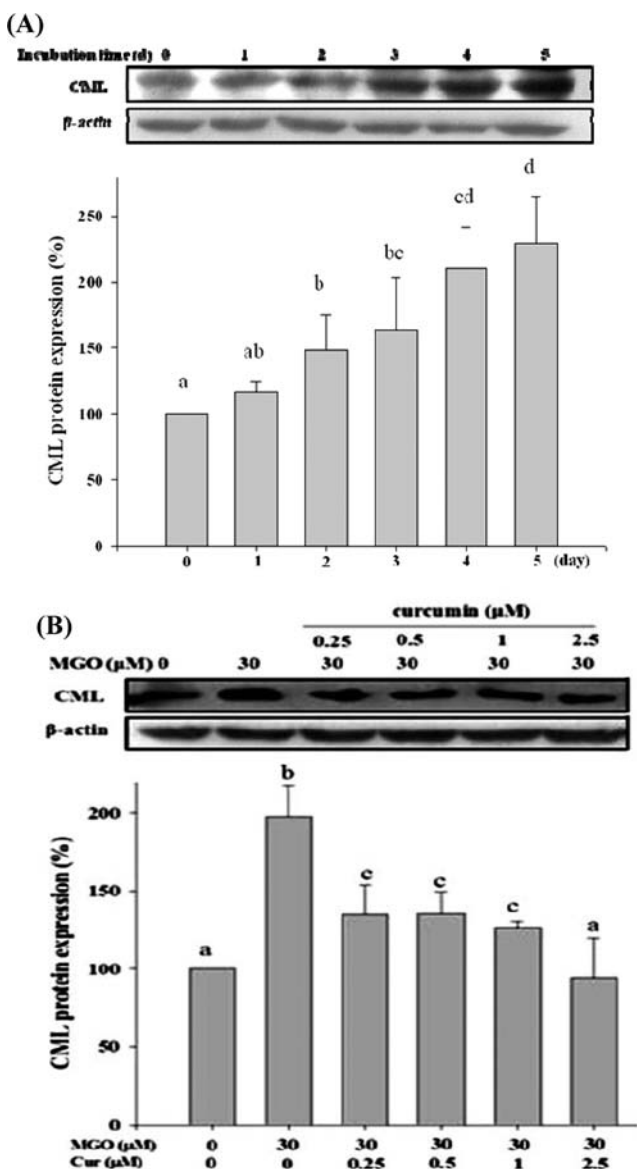


Figure 8. Effect of MGO (30 μ M) on the protein level of CML in HUVECs during incubation for 5 days (A). Effect of curcumin pretreatment (24 h) followed by incubation with MGO (30 μ M) for 4 days on the protein level of CML in HUVECs (B). Values are means \pm SD, $n = 3$; means without a common letter differ significantly, $P < 0.05$.

fragment ion m/z 175 ($[M - 192 - H]^-$) by ring-closure reaction from deprotonated curcumin.²⁶

Several lines of evidence support that peak 1 is a curcumin-like compound. First, the molecular ion of peak 1 is m/z 439 ($[M - H]^-$), which may lose one molecule of H_2O to generate the fragment ion m/z 421 ($[M - 18 - H]^-$) and subsequently lose a neutral moiety to form fragment ion m/z 271 ($[M - 18 - 150 - H]^-$) (Table 1), suggesting that peak 1 undergoes the same degradation as does curcumin. Second, the UV maximal absorbances for peak 1 were 429, 275, and 236 nm, which are similar to those of curcumin (Table 1). Moreover, the molecular weight of peak 1 was 440, which equals the molecular weight of MGO (72) plus that of curcumin (368) (Table 1). Thus, it is reasonable to speculate that peak 1 is a curcumin–MGO adduct. However, peak 2 is unlikely to be di-MGO or tri-MGO adducts of curcumin because the molecular

ion of peak 2 is m/z 549 ($[M - H]^-$), which should lose a weight of 180 to generate the fragment ion m/z 369 ($[M - 180 - H]^-$) (Table 1). In addition, the molecular weight of di-MGO ($72 \times 2 = 144$) or tri-MGO ($72 \times 3 = 216$) is different from 180. Further study is needed to identify peak 2, an unknown compound.

Curcumin Traps MGO by Its Diketone Group, but Not by Its Phenol Groups. We then used two curcumin analogues, DIMC and ferulic acid, to determine whether the MGO-trapping site of curcumin is its diketone group or phenol groups. The structure of DIMC contains two methoxy groups, rather than one methoxy group, and one hydroxyl group in each of the two benzene moieties in curcumin (Figure 1). The structure of ferulic acid, a half-structure of curcumin, has a carboxylic group rather than ketone group (Figure 1). By reacting 0.48 mM DIMC or 0.48 mM ferulic acid with 1.45 mM MGO (i.e., a 1:3 ratio) at 37 $^{\circ}$ C for 24 h, we found that DIMC reduced the level of MGO by 31% (Figure 4A), which is equivalent to one DIMC molecule trapping one MGO molecule (i.e., (1.45 mM MGO \times 31%)/0.48 mM DIMC) (Figure 4B). Notably, the reduced MGO level and the MGO-trapping ratio of DIMC are equivalent to those of curcumin (Figure 4). In contrast, ferulic acid did not trap MGO (\sim 0.7%) even though there is a hydroxyl group (C3) in its benzene moiety, which could render C4 a high electron density carbon under alkaline conditions. Previous reports have revealed that EGCG has two hydroxyl groups (C5 and C7) with meta substitution on the A ring and two unsubstituted carbons (C6 and C8), which can react with MGO owing to the high electron density upon dissociation of a hydrogen atom from two hydroxyl groups under alkaline conditions.^{3,28} Unlike EGCG, ferulic acid has only one hydroxyl group in the benzene moiety, but the electron density of the C4 carbon of ferulic acid may not be strong enough to trap MGO. Thus, the phenol structure of curcumin, like that of ferulic acid, fails to trap MGO at the unsubstituted carbons (C4) of the benzene rings.

Another functional group of curcumin is the β -diketone group. The two hydrogen atoms on the carbon (C10) between the two keto carbons are quite acidic and can be converted completely to enolate anions under alkaline conditions.³³ Moreover, the negative charge on the oxygen atom is shared by the carbon atoms between the two β -diketones through resonance, making this carbon atom (C10) a nucleophile. In addition, the pK_a of hydrogen (\sim 9) on the carbon between the two keto carbons is lower than that (\sim 10) of the hydroxyl group of phenol,³³ therefore, this carbon between the β -diketone is more prone to losing a H^+ ion. On the basis of these observations and the evidence from the literature, we reasonably speculate that the nucleophilicity of the carbon atom (C10) between the two keto carbons facilitates the addition of MGO at this position (Figure 5) to form a mono-MGO adduct of curcumin by the reaction of curcumin with MGO at a 1:3 ratio.

Curcumin Decreases Intracellular MGO Levels in HUVECs Incubated with MGO. Curcumin at low concentrations (0–2.5 μ M) did not affect cell proliferation at 12 and 24 h of incubation (Figure 6). In contrast, curcumin at higher concentrations (5–20 μ M) significantly inhibited cell proliferation; for instance, curcumin at 20 μ M inhibited proliferation by 55% ($P = 0.001$) and 57% ($P = 0.001$) at 12 and 24 h of incubation, respectively. Therefore, we chose a preincubation time of 24 h and 0.25–2.5 μ M curcumin for the following studies. Since curcumin traps MGO under physio-

logical conditions, we further determined the effects of curcumin on the MGO-trapping capacity in HUVECs. We found that incubation of HUVECs with exogenously added MGO (30 μM) for up to 5 days significantly increased intracellular MGO levels and that this effect was the strongest on the third day of incubation (by 3-fold, $P < 0.05$), after which the effect weakened slightly at 4–5 days of incubation (Figure 7A). In addition, pretreatment of HUVECs with curcumin (0.25–2.5 μM) for 24 h significantly reduced the levels of intracellular MGO induced by exogenous MGO on the third day of incubation (Figure 7B).

Elevated levels of MGO cause carbonyl stress and irreversibly modify lysine and arginine residues of protein to form AGEs in vivo.³⁴ It has been shown that MGO-derivatized CML is the most abundant AGE in proteins.³⁵ We found that exogenous MGO (30 μM) significantly increased protein expression of CML in HUVECs during 5 days of incubation and that the effect was the strongest on the fourth and fifth days of incubation (by 2.1- and 2.3-fold, respectively, $P < 0.05$) (Figure 8A). Pretreatment of HUVECs with curcumin (0.25–2.5 μM) for 24 h ameliorated the exogenous MGO-induced CML formation in a concentration-dependent manner on the fourth day of incubation (Figure 8B). Thus, curcumin not only effectively trapped MGO in a cell-free system but also decreased the exogenous MGO-induced levels of intracellular MGO and protein expression of CML in HUVECs, indicating that curcumin can inhibit the formation of AGEs through its MGO-trapping capacity.

In conclusion, we have shown that curcumin is an efficient MGO-trapping agent in the cell-free system as well as in HUVECs, leading to decreased CML expression. In addition, we demonstrate that the major active site of curcumin is at the carbon atom (C10) between the two keto carbons, which can trap one molecule of MGO to form a curcumin–MGO adduct. These results support the notion that AGE inhibitors from natural foodstuffs may be potential therapeutic agents for delaying and preventing diabetic complication.

AUTHOR INFORMATION

Corresponding Author

*Phone: +886-4-2631-8652, ext 5602 (C.-C.C.); +886-4-2281-2363 (M.-L.H.). Fax: +886-4-2281-2363 (M.-L.H.). E-mail: ccchayau@sunrise.hk.edu.tw (C.-C.C.); mlhuhu@nchu.edu.tw (M.-L.H.).

Author Contributions

[†]T.-Y.H. and C.-L.L. contributed equally to this work.

Funding

This work was supported in part by the Ministry of Education, Taiwan, ROC, under the ATU plan.

Notes

The authors declare no competing financial interest.

REFERENCES

- (1) The Diabetes Control and Complications Trial Research Group. The effect of intensive treatment of diabetes on the development and progression of long-term complications in insulin-dependent diabetes mellitus. *N. Engl. J. Med.* **1993**, *329* (14), 977–86.
- (2) Brownlee, M.; Cerami, A.; Vlassara, H. Advanced glycosylation end products in tissue and the biochemical basis of diabetic complications. *N. Engl. J. Med.* **1988**, *318* (20), 1315–21.
- (3) Sang, S.; Shao, X.; Bai, N.; Lo, C. Y.; Yang, C. S.; Ho, C. T. Tea polyphenol (-)-epigallocatechin-3-gallate: a new trapping agent of

reactive dicarbonyl species. *Chem. Res. Toxicol.* **2007**, *20* (12), 1862–70.

(4) Wu, C. H.; Huang, S. M.; Lin, J. A.; Yen, G. C. Inhibition of advanced glycation endproduct formation by foodstuffs. *Food Funct.* **2011**, *2* (5), 224–34.

(5) Shibamoto, T. Analytical methods for trace levels of reactive carbonyl compounds formed in lipid peroxidation systems. *J. Pharm. Biomed. Anal.* **2006**, *41* (1), 12–25.

(6) Aldini, G.; Dalle-Donne, I.; Facino, R. M.; Milzani, A.; Carini, M. Intervention strategies to inhibit protein carbonylation by lipoxidation-derived reactive carbonyls. *Med. Res. Rev.* **2007**, *27* (6), 817–68.

(7) Beisswenger, P. J.; Howell, S. K.; Nelson, R. G.; Mauer, M.; Szwegold, B. S. Alpha-oxoaldehyde metabolism and diabetic complications. *Biochem. Soc. Trans.* **2003**, *31* (Part6), 1358–63.

(8) Khuhawar, M.; Kandhro, A.; Khand, F. Liquid chromatographic determination of glyoxal and methylglyoxal from serum of diabetic patients using meso-stilbenediamine as derivatizing reagent. *Anal. Lett.* **2006**, *39* (10), 2205–2215.

(9) Kalapos, M. P. Methylglyoxal in living organisms: chemistry, biochemistry, toxicology and biological implications. *Toxicol. Lett.* **1999**, *110* (3), 145–75.

(10) Turk, Z. Glycotoxines, carbonyl stress and relevance to diabetes and its complications. *Physiol. Res.* **2010**, *59* (2), 147–56.

(11) Lyles, G. A.; Chalmers, J. The metabolism of aminoacetone to methylglyoxal by semicarbazide-sensitive amine oxidase in human umbilical artery. *Biochem. Pharmacol.* **1992**, *43* (7), 1409–14.

(12) Casazza, J. P.; Felver, M. E.; Veech, R. L. The metabolism of acetone in rat. *J. Biol. Chem.* **1984**, *259* (1), 231–6.

(13) Frye, E. B.; Degenhardt, T. P.; Thorpe, S. R.; Baynes, J. W. Role of the Maillard reaction in aging of tissue proteins. Advanced glycation end product-dependent increase in imidazolium cross-links in human lens proteins. *J. Biol. Chem.* **1998**, *273* (30), 18714–9.

(14) Ahmed, M. U.; Brinkmann Frye, E.; Degenhardt, T. P.; Thorpe, S. R.; Baynes, J. W. N-epsilon-(carboxyethyl)lysine, a product of the chemical modification of proteins by methylglyoxal, increases with age in human lens proteins. *Biochem. J.* **1997**, *324* (Part 2), 565–70.

(15) Shipanova, I. N.; Glomb, M. A.; Nagaraj, R. H. Protein modification by methylglyoxal: chemical nature and synthetic mechanism of a major fluorescent adduct. *Arch. Biochem. Biophys.* **1997**, *344* (1), 29–36.

(16) Aggarwal, B. B.; Sundaram, C.; Malani, N.; Ichikawa, H. Curcumin: the Indian solid gold. *Adv. Exp. Med. Biol.* **2007**, *595*, 1–75.

(17) Reddy, A. C.; Lokesh, B. R. Effect of dietary turmeric (*Curcuma longa*) on iron-induced lipid peroxidation in the rat liver. *Food Chem. Toxicol.* **1994**, *32* (3), 279–83.

(18) Zhang, F.; Altorki, N. K.; Mestre, J. R.; Subbaramaiah, K.; Dannenberg, A. J. Curcumin inhibits cyclooxygenase-2 transcription in bile acid- and phorbol ester-treated human gastrointestinal epithelial cells. *Carcinogenesis* **1999**, *20* (3), 445–51.

(19) Duvoix, A.; Morceau, F.; Delhalle, S.; Schmitz, M.; Schnekenburger, M.; Galteau, M. M.; Dicato, M.; Diederich, M. Induction of apoptosis by curcumin: mediation by glutathione S-transferase P1–1 inhibition. *Biochem. Pharmacol.* **2003**, *66* (8), 1475–83.

(20) Suryanarayana, P.; Saraswat, M.; Mrudula, T.; Krishna, T. P.; Krishnaswamy, K.; Reddy, G. B. Curcumin and turmeric delay streptozotocin-induced diabetic cataract in rats. *Invest. Ophthalmol. Visual Sci.* **2005**, *46* (6), 2092–9.

(21) Jain, S. K.; Rains, J.; Jones, K. Effect of curcumin on protein glycosylation, lipid peroxidation, and oxygen radical generation in human red blood cells exposed to high glucose levels. *Free Radical Biol. Med.* **2006**, *41* (1), 92–6.

(22) Mosmann, T. Rapid colorimetric assay for cellular growth and survival: application to proliferation and cytotoxicity assays. *J. Immunol. Methods* **1983**, *65* (1–2), 55–63.

(23) Lo, C. Y.; Li, S.; Tan, D.; Pan, M. H.; Sang, S.; Ho, C. T. Trapping reactions of reactive carbonyl species with tea polyphenols in simulated physiological conditions. *Mol. Nutr. Food Res.* **2006**, *50* (12), 1118–28.

(24) Peng, X.; Cheng, K. W.; Ma, J.; Chen, B.; Ho, C. T.; Lo, C.; Chen, F.; Wang, M. Cinnamon bark proanthocyanidins as reactive carbonyl scavengers to prevent the formation of advanced glycation endproducts. *J. Agric. Food Chem.* **2008**, *56* (6), 1907–11.

(25) Peng, C. H.; Chiu, W. T.; Juan, C. W.; Mau, J. L.; Chen, C. C.; Peng, C. C.; Lai, E. Y.; Chyau, C. C. Pivotal role of curcuminoids on the antimutagenic activity of *Curcuma zedoaria* extracts. *Drug Chem. Toxicol.* **2010**, *33* (1), 64–76.

(26) Jiang, H.; Somogyi, A.; Jacobsen, N. E.; Timmermann, B. N.; Gang, D. R. Analysis of curcuminoids by positive and negative electrospray ionization and tandem mass spectrometry. *Rapid Commun. Mass Spectrom.* **2006**, *20* (6), 1001–12.

(27) Dhar, A.; Desai, K.; Liu, J.; Wu, L. Methylglyoxal, protein binding and biological samples: are we getting the true measure? *J. Chromatogr., B: Anal. Technol. Biomed. Life Sci.* **2009**, *877* (11–12), 1093–100.

(28) Shao, X.; Bai, N.; He, K.; Ho, C. T.; Yang, C. S.; Sang, S. Apple polyphenols, phloretin and phloridzin: new trapping agents of reactive dicarbonyl species. *Chem. Res. Toxicol.* **2008**, *21* (10), 2042–50.

(29) Peng, X.; Ma, J.; Chao, J.; Sun, Z.; Chang, R. C.; Tse, I.; Li, E. T.; Chen, F.; Wang, M. Beneficial effects of cinnamon proanthocyanidins on the formation of specific advanced glycation endproducts and methylglyoxal-induced impairment on glucose consumption. *J. Agric. Food Chem.* **2010**, *58* (11), 6692–6.

(30) Liu, H.; Gu, L. Phlorotannins from brown algae (*Fucus vesiculosus*) inhibited the formation of advanced glycation endproducts by scavenging reactive carbonyls. *J. Agric. Food Chem.* **2012**, *60* (5), 1326–34.

(31) Lv, L.; Shao, X.; Wang, L.; Huang, D.; Ho, C. T.; Sang, S. Stilbene glucoside from *Polygonum multiflorum* Thunb.: a novel natural inhibitor of advanced glycation end product formation by trapping of methylglyoxal. *J. Agric. Food Chem.* **2010**, *58* (4), 2239–45.

(32) van Baar, B. L. M.; Rozendal, J.; van der Goot, H. Electron ionization mass spectrometry of curcumin analogues: an olefin metathesis reaction in the fragmentation of radical cations. *J. Mass Spectrom.* **1998**, *33* (4), 319–327.

(33) Marye, A. Fox, J. k. W. *Organic Chemistry*, 3rd ed.; Jones & Bartlett Learning: Burlington, MA, 2004.

(34) Desai, K. M.; Wu, L. Free radical generation by methylglyoxal in tissues. *Drug. Metab. Drug Interact.* **2008**, *23* (1–2), 151–73.

(35) Huang, S. M.; Hsu, C. L.; Chuang, H. C.; Shih, P. H.; Wu, C. H.; Yen, G. C. Inhibitory effect of vanillic acid on methylglyoxal-mediated glycation in apoptotic Neuro-2A cells. *Neurotoxicology* **2008**, *29* (6), 1016–22.